C. J. Deepu; C. H. Heng; Y. Lian, "A Hybrid Data Compression Scheme for Power Reduction in Wireless Sensors for IoT," in IEEE Transactions on Biomedical Circuits and Systems , vol.PP, no.99, pp.1-10 doi: 10.1109/TBCAS.2016.2591923

A Hybrid Data Compression Scheme for Power Reduction in Wireless Sensors for IoT

Chacko John Deepu, *Senior Member, IEEE*, Chun-Huat Heng, *Senior Member, IEEE*, and Yong Lian, *Fellow, IEEE*

***Abstract*—This paper presents a novel data compression and transmission scheme for power reduction in Internet-of-Things (IoT) enabled wireless sensors. In the proposed scheme, data is compressed with both lossy and lossless techniques, so as to enable *hybrid transmission mode*, support adaptive data rate selection and save power in wireless transmission. Applying the method to electrocardiogram (ECG), the data is first compressed using a lossy compression technique with a high compression ratio (CR). The residual error between the original data and the decompressed lossy data is preserved using entropy coding, enabling a lossless restoration of the original data when required. Average CR of 2.1× and 7.8× were achieved for lossless and lossy compression respectively with MIT/BIH database. The power reduction is demonstrated using a Bluetooth transceiver and is found to be reduced to 18% for lossy and 53% for lossless transmission respectively. Options for *hybrid transmission mode*, adaptive rate selection and system level power reduction make the proposed scheme attractive for IoT wireless sensors in healthcare applications.**

***Index Terms*—Hybrid compression, internet-of-things, lossless, lossy, wearable devices, wireless sensors.**

I. Introduction

THE rapidly increasing healthcare expenditure worldwide has triggered a renewed interest in developing personal healthcare systems. Cardiovascular diseases, which are the leading contributors to this expenditure, can be proactively managed using Internet-of-Things (IoT) enabled wearable electrocardiogram (ECG) sensors. The use of wireless wearable sensors in cardio-patients reduces healthcare costs and leads to better overall quality of life. The main challenge involved in the development of a wearable sensor is the design of an ultra-low power integrated circuit which can acquire, process and wirelessly transmit physiological signals to a remote monitoring centre [1]. A high level of integration with built in signal acquisition and data conversion is required to minimize the size, cost and power consumption of such a sensor [2].

Manuscript received December 15, 2015; revised April 21, 2016 and June 26, 2016; accepted July 1, 2016. This work was supported in part by the National Research Foundation Singapore under Grant NRF-CRP8-2011-01 and Natural Sciences and Engineering Research Council of Canada Discovery Grant. This paper was recommended by Associate Editor K. Chakrabarty.

C. J. Deepu and C.-H. Heng are with the Department of Electrical and Computer Engineering, National University of Singapore, Singapore (e-mail: deepu.john@ieee.org).

Y. Lian is with the Department of Electrical Engineering and Computer Science of Lassonde School of Engineering, York University, Toronto, ONM3J 1P3, Canada (e-mail: plian@yorku.ca).

Color versions of one or more of the figures in this paper are available online at http://ieeexplore.ieee.org.

Digital Object Identifier 10.1109/TBCAS.2016.2591923

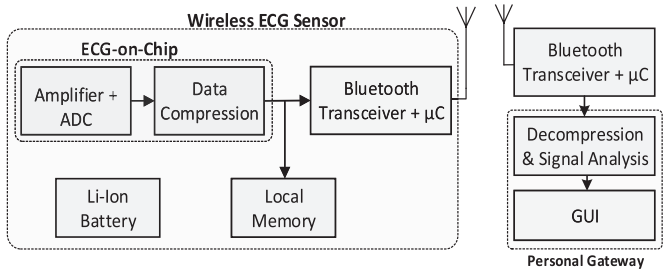

Fig. 1. Wireless ECG monitoring system.

In typical wearable ECG sensor, as in Fig. 1, the wireless transceiver is the major source of power consumption (up to 90%) [3], [4]. Further, the large quantity of data obtained by round the clock monitoring may need to be either stored in a local memory (Flash/RAM) or transmitted wirelessly to a gateway device for further analysis. The transmission of data incurs high energy consumption, and the use of a large local storage increases the device cost [5]. A custom made wireless transceiver may be able to fix the power consumption issue, but will lose interoperability with the billions of smart devices already shipped with Bluetooth and therefore limits its adoption rate. Furthermore, the newly introduced Bluetooth Smart has limited data rate. Therefore, it is desirable to introduce a data compression scheme at the sensor, so as to reduce the amount of data that needs to be transmitted or stored. This can reduce the system level power consumption and memory resource requirements while being able to use the existing radios like Bluetooth and Bluetooth Smart.

Many recent literatures on sensor data compression focus on lossy compression, compressed sensing, adaptive/continuous time sampling methods [6]–[8]. This is because such techniques traditionally provide better compression ratio (CR) of 2–15 times, compared to lossless techniques which gives 1–3 times CR. The quality of ECG signal from lossy compression in most cases may be acceptable for clinical use. However, the medical regulatory standards used in most countries does not explicitly endorse the usage of lossy compression techniques in commercial devices [9], [10]. This is because of the uncertainty, that if all the patient data of potential diagnostic value can be fully retained by such techniques. Also in adaptive or continuous time sampling systems, data cannot be stored in memory for future use as there is no reference for time [11]. Due to these issues, much effort has been recently invested in lossless techniques [12]–[14], [31] which achieved good energy efficiency and CR.

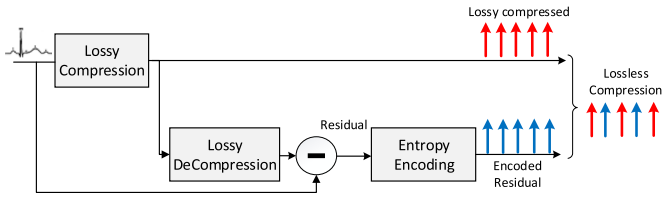

Fig. 2. Block diagram of proposed hybrid scheme.

In this paper, we present a novel scheme that addresses the issues in compression performance, system level power consumption and ECG signal quality. What we propose is a hybrid context aware compression and transmission scheme, which enables *hybrid lossless transmission*, power aware data rate selection and is tailored to the context of a battery operated wearable low cost device. The sensor data is compressed in both lossy and lossless fashion to facilitate hybrid and context aware data transmission. The lossy compressed data achieves 7.8x compression with an RMS error of 4.6 and Percentage RMS difference (PRD) of 0.51%. The lossless scheme achieves a CR of 2.1x with minimal additional hardware complexity. The proposed scheme is synthesized in 0.35 μm CMOS process and consumes only 260 nW with 4 K gate complexity. Ultra-low power consumption, small size and real time data rate selection capability makes the proposed technique well suited for wireless sensors in IoT applications.

This paper is organized as follows. In Section II, the proposed scheme is detailed. The selection of compression algorithms to serve as the engine of hybrid compression scheme are presented in Section III. The performance evaluation and hardware architecture are discussed in Sections IV and V. A prototype system is illustrated in Section VI for verifying the proposed scheme. Conclusions are given in Section VII.

II. Proposed Data Compression Scheme

The proposed data compression scheme is a hybrid of lossy and lossless compressions, as shown in Fig. 2. It consists of a lossy compression block, a lossy decompression unit and an entropy encoder.

The ECG data is first compressed by a lossy compression technique, which has a high CR of 6–10x. At this CR, the reconstructed data typically attains acceptable PRD (ref. to Table III). The lossy compressed data forms one of the outputs of the compression unit, whose quality is sufficient for preliminary assessment of QRS peak location, heart rate variability (HRV) etc.

In cases where a more comprehensive signal analysis is required, the original ECG is reconstructed using a lossless compressed data stream from the bottom branch in Fig. 2, i.e., the residual error between the decompressed lossy data and original data is calculated and entropy encoded to generate another output. Note that the residual error has a very low dynamic range and the entropy encoding helps to minimize the bit-rate. The lossy compressed signal along with encoded residuals can fully represent the original signal in a lossless fashion. Fig. 3 illustrates the original signal, reconstructed lossy signal and residual error. Fig. 4 shows the spectrum of the original/lossless and lossy reconstructed signal. It can be

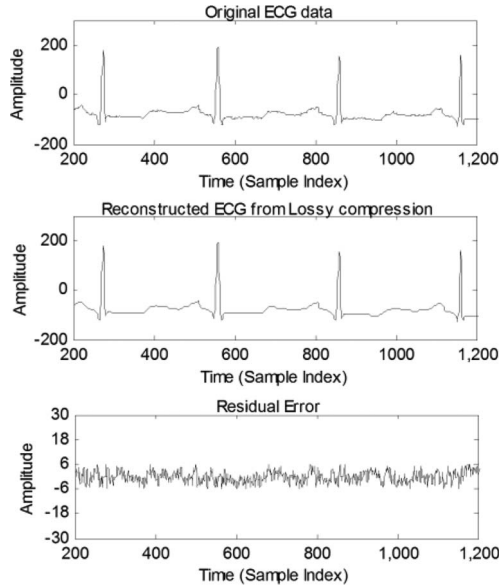

Fig. 3. Reconstructed lossy signal and residual error.

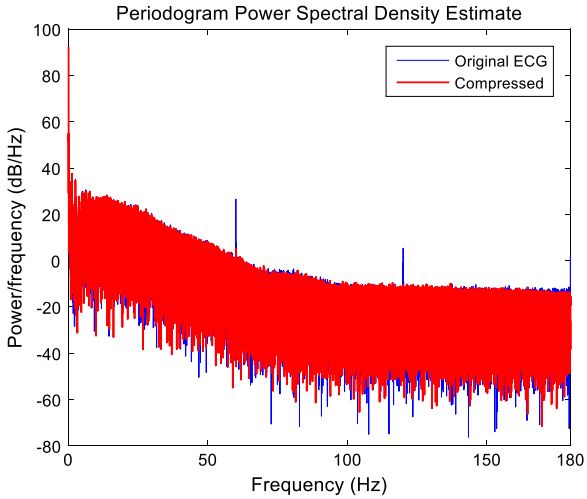

Fig. 4. Frequency spectrum of compressed versus original signal.

observed that the lossy compression has very minimal impact on the signal except that it slightly attenuates the high frequency content.

While decompressing, a lossy reconstruction of the signal is done first, followed by addition of decoded residual error of the corresponding sample to achieve lossless decompression. The hybrid scheme shares the computational complexity of lossy coding with lossless coding.

The proposed scheme has several unique advantages over traditional lossless schemes in the context of wearable devices as highlighted below.

1) Enabling Hybrid Transmission Mode: The most unique advantage of the proposed technique is that it enables ***hybrid transmission mode*** in wireless sensors [shown in Fig. 5(a), (b)] to help reduce the overall power consumption. Here, in normal operation only the lossy compressed data is transmitted wirelessly in real-time and the corresponding residual is stored in

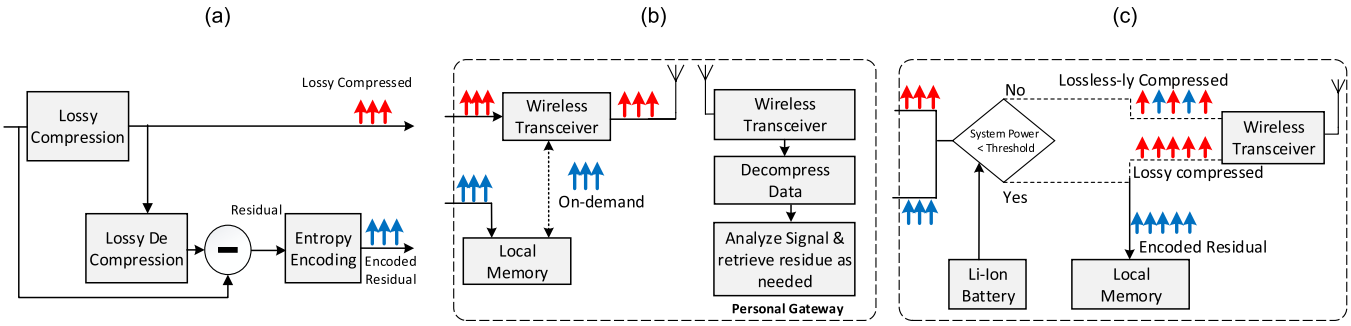

Fig. 5. (a) Hybrid compression. (b) Hybrid lossless transmission. (c) Power aware transmission.

local memory. This enables more than 80% savings in power in the wireless transmitter and thus significantly extends the sensor battery life. In most cases, the fidelity of the reconstructed data from lossy compression is adequate for preliminary signal analysis. To verify this, we tested QRS peak detection from lossy compressed ECG data against the results obtained from [15]. Using 5 records from the MIT/BIH database, it was found that the detection accuracy is reduced by only a nominal 0.06% for the lossy data [16]. Typically, the gateway carries out preliminary signal processing tasks such as QRS and atrial-fibrillation detection. The gateway may also choose to dynamically adjust the CR based on patient condition, i.e., to program the sensor to increase or decrease the signal precision to change data rate. In case an abnormality is observed in the results, the gateway can request to receive raw ECG data by retrieval of the stored residual data from the sensor for a lossless restoration and a more precise analysis. In most cases, the occurrence of an abnormal heart rhythm is very infrequent and therefore this scheme results in overall improvement in system level power consumption. The residual data can be also retrieved wirelessly while the sensor is docked for charging to enable a lossless restoration of raw data to be stored in a database. The proposed *hybrid transmission mode* is useful to reduce power consumption in any IoT wireless application, where a less precise data can be used for preliminary analysis.

2) Enabling Power Aware Transmission: Most IoT devices are battery powered, and therefore a sudden and abrupt end of data acquisition and transmission occurs when the battery drains out [17], [18].

A typical lossless compression scheme with CR $>$ 2x can extend the battery life by around 2 times. A further improvement in sensor functionality can be obtained by enabling graceful data degradation using the proposed compression scheme, i.e., when the projected battery life of the device falls below a minimum threshold (say 20%), the device can switch to lossy only transmission mode instead of a fully lossless transmission, extending the battery life of the device as shown in Fig. 5(a), (c). The remaining battery life is typically measured by sampling the present battery output voltage levels. The savings can be validated based on the results from Table V. The encoded residual data during this time can be locally stored or discarded.

3) Optimizing Utilization of Local Storage: The data acquired from the ECG sensor is typically stored in a local memory. Round the clock acquisition of multi-lead ECG requires a large local storage. For example, an 8-channel 12-bit ECG recording at 1 kHz would require 1.04 Gigabytes of storage per day. Only limited memory can be embedded in a sensor to maintain low cost. A hybrid compression scheme with adaptive data rate selection enables the tradeoff between limited memory resources and data quality, by storing only lossy data when the remaining memory is limited (say 20%).

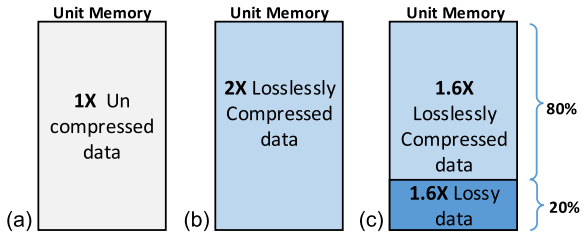

Fig. 6. Data stored in a unit memory with (a) no compression, (b) lossless compression, and (c) hybrid scheme with lossless for first 80% and lossy for 20% storage.

An illustration of memory usage assuming a lossless CR of 2x and lossy CR of 8x is given in Fig. 6. Assuming 1-unit memory device can store 1x uncompressed data, it can store up to 3.2x data in hybrid compression mode. This has been validated with 2 records (Tapes 108 & 112) from MIT database. It is observed that hybrid storage mode can store up to 2.96 and 3.62 times their equivalent raw data.

4) Increased Error Tolerance: Lossless compression schemes typically use linear predictive coding techniques to remove the redundancy between neighboring data samples [13], [19]. Thus, only the uncorrelated part of the signal is stored or transmitted resulting in data compression. However, when intermediate packets are lost due to bad channel conditions in wireless transmission or due to damaged sectors in a memory device, the entire data can become un-decodable. Currently, such issues are accounted for by sending periodic re-syncing frames with full data samples [12].

A high frequency of re-syncing frames ensures a fast recovery after a packet loss, at the expense of compression ratios. Even then, a full data recovery cannot be made until the next re-syncing frame. By using the proposed hybrid data compression scheme, where the data is compressed as lossy and the residual is compressed as lossless, a fast restoration of data can be ensured in case of a total packet loss, as illustrated in Fig. 7. Also, a high error resilient transmission of the lossy data using the Forward Error Correction (FEC), Automatic Repeat Request (ARQ) schemes ensure that at least some level of data

Fig. 7. Illustration of higher error tolerance with wireless sensors.

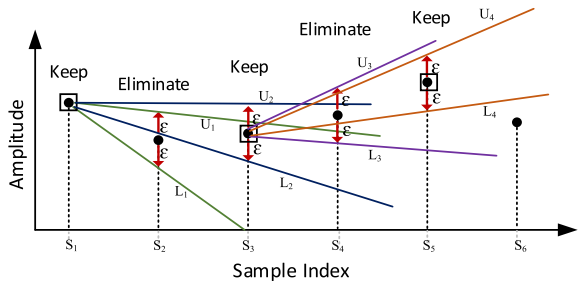

Fig. 8. Fan algorithm illustration.

restoration can be achieved in the receiver even in the case of an extremely noisy channel.

III. Hybrid Scheme Implementation

The proposed hybrid compression scheme will work with any existing lossy and lossless compression/decompression algorithms. However, the implementation complexity is highly depended on the choice of lossy compression and decompression schemes. This is because the lossy compressed data must be decompressed locally at the sensor node for generating residual error. Any lossy technique with a complex reconstruction scheme is not favored for the proposed approach due to the limited computational resources available in an IoT sensor node. A review of several lossy compression techniques is given in [20]. Popular lossy compression techniques, such as those that rely on quantization or sub-sampling of the ECG data to obtain a coarser version of the actual data, are not the best candidate for proposed scheme. The uniform subsampling methods, such as simple decimation, guarantee a desired compression ratio, but they may not preserve signal fidelity well. On the other hand, the non-uniform sub-sampling techniques, such as Fan compression algorithm [20], are more effective in retaining signal fidelity as compared to uniform sub-sampling. In addition, Fan is simple for hardware implementation (as discussed in Section V) compared to transform domain based techniques [21], [22]. That is because Fan algorithm implementation does not require complex filter banks or memory elements like transform domain compression methods [23]. Thus, we selected Fan for demonstrating the proposed scheme. In the next subsections, we will first review the Fan algorithm for better understanding of implementation scheme presented in Section V, and followed by the discussion on optimizing the Fan algorithm parameters for proposed scheme. The performance evaluation is presented for the proposed hybrid scheme using a combination of Fan algorithm and Huffman coding.

1) Fan Algorithm: Fan algorithm is an adaptive sub-sampling approach, that operates by drawing the longest possible straight line between the starting sample and the ending sample, in such a way that the error in reconstruction of the intermediate samples are less than the maximum specified error value, ε. Fan algorithm is illustrated in Fig. 8.

The algorithm is initialized by storing the first sample, S_1, permanently, which serves as the first origin point. For the next sample S_2, two different bounds are computed as amplitude of $S_2 \pm \varepsilon$. Two different slopes (U_1, L_1) are drawn between the origin point and the upper $(S_2 + \varepsilon)$ and lower $(S_2 - \varepsilon)$ bound. If the amplitude of the next sample (S_3) is within the bounds created by slopes (U_1, L_1) at S_3, then sample S_2 is eliminated. The process continues with computing the upper and lower error bounds of sample $S_3(S_3 \pm \varepsilon)$. From the origin point S_1, two new slopes (U_2, L_2) are drawn to the points $(S_3 + \varepsilon)$ and $(S_3 - \varepsilon)$. These new slopes are compared with the previous slopes (U_1, L_1) and most converging slopes are retained, i.e., (U_1, L_2) in the illustration. Since the amplitude of the next sample S_4 does not fall within the bounds created by slopes (U_1, L_2), the sample just before that, i.e., S_3, is retained for storage and is made as the next origin point and the process is repeated for all the remaining samples. The duration between 2 consecutive samples, which are retained by the algorithm, is stored as a field *length* to each retained sample. The decompression will be done by simple linear interpolation.

ECG signals compressed/decompressed by the Fan algorithm at different ε values in Matlab are shown in Fig. 9. The residual error, computed by subtracting the lossy-reconstructed signal from original signal, centers on zero and its maximum value is bounded by the ε valued used.

2) Residual Encoding With Huffman Coding: Huffman coding, which associates the most frequently occurring symbols with short codewords and the less frequently occurring symbols with long codewords, will reduce the overall bit-rate further since majority of the residual error samples are centred on zero (Fig. 10). This symbol-codeword association table is pre-constructed using a statistical dataset. Since there is only limited number of error symbols in this case (i.e., bounded by ε), it can be simply implemented using a lookup table.

3) Reconstruction of Original Data: For reconstruction of original lossless data, the lossy data is reconstructed first using linear interpolation. Further, the residual samples have to be synchronized with the lossy reconstructed data based on the *length* field which is the duration between consecutive samples.

IV. Optimization & Performance Evaluation

The performance of Fan compression in itself has been analyzed before in [20]–[22]. The main focus of the previous studies is to achieve a higher CR with given constraints. However, for the proposed hybrid method, lossy and lossless performance has to be jointly evaluated and optimized in order to achieve better energy efficiency and low hardware cost. To find the optimum performance point of Fan algorithm for the proposed hybrid scheme, the overall compression performance is analysed against different maximum residual error amplitude levels that corresponds to 0.1–1% of the dynamic range of the

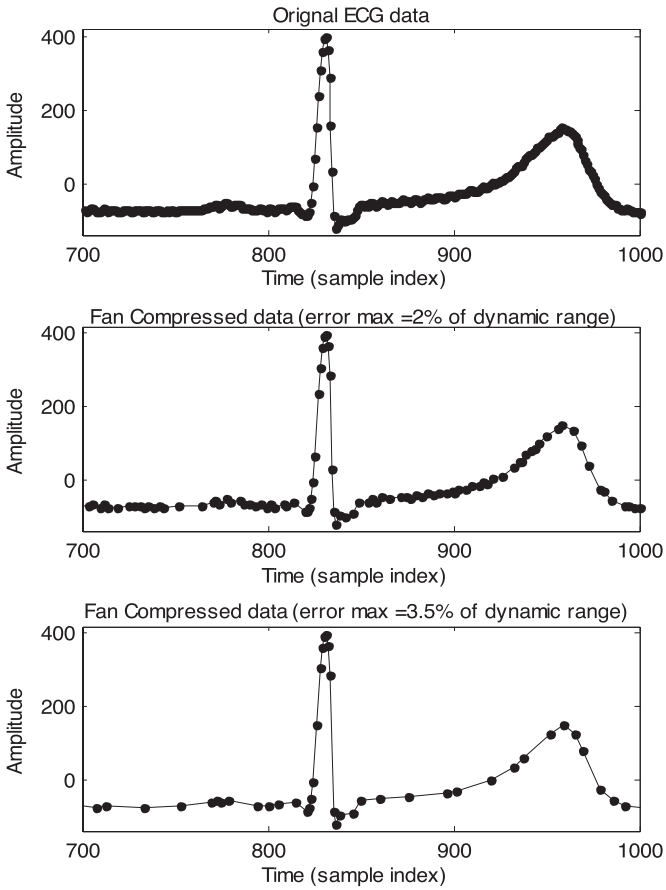

Fig. 9. Fan compressed signals with different error levels.

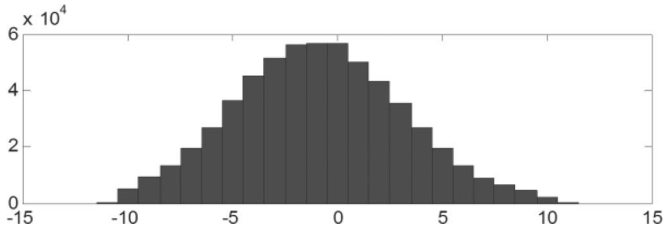

Fig. 10. Residual error probability histogram with $\varepsilon = 10$.

ECG signal. We use the records from MIT/BIH Arrhythmia Database [16] as test datasets, which are digitized at 11-bit resolution. With 11-bit resolution, the maximum residual error of 0.1–1% of the dynamic range limits the error to absolute values between 2∼20. Fig. 11 shows the average compression performance of the algorithm for 48 half hour MIT ECG tapes at different allowed error levels. For lossy compression, the relationship between CR and maximum allowed residual error amplitude is linear as expected. As the maximum allowed error is increased, more samples are dropped, which results in a higher compression ratio.

For lossless compression, it is obvious from Fig. 11 that there is an optimum CR value associated with residual error levels, which is around 2.1. This is due to following two reasons. First, at very low error levels, only a few samples are dropped by the Fan compression and the remaining samples have the additional

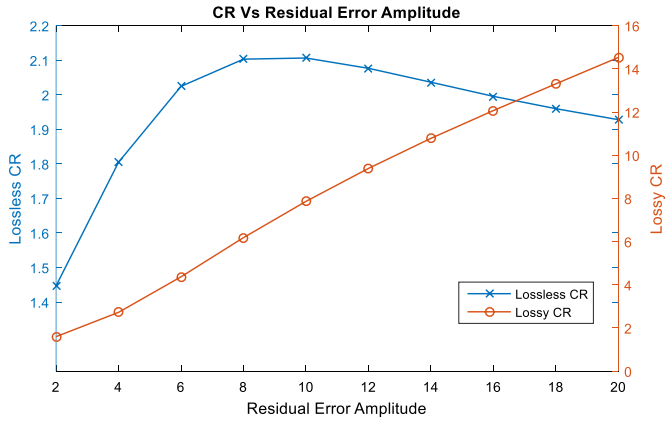

Fig. 11. Residual error versus lossless compression ratio.

overhead of appending the "*length*" field, which denotes the duration from the previous sample. Second, as error levels are increased, more samples are skipped, and the influence of the "*length*" field overhead is minimal. This leads to the best performance. Third, at higher maximum allowed error levels, the variance of the residual error distribution is increased. This results in the need for a higher bit width representation in encoding the residual error, i.e., more bits are needed for Huffman coding (which will be presented in next section). Hence overall CR decreases. From the simulation results (Fig. 11), it is clear that the residual error levels should be limited to the range between 0.3–0.7% of the maximum dynamic range of the signal for optimal performance.

By using the optimized residual error levels, the performance of the proposed scheme is evaluated based on RMS error (RMSE), PRD and CR, which are the commonly used figures of merits (FOM) for lossy compression and is given in (1) to (3), respectively. RMSE has the same unit as of $x(n)$, i.e., amplitude in analog to digital converter (ADC) units. CR alone is the FOM for the lossless method.

$$\text{PRD} = \sqrt{\frac{\sum_n \left(x(n) - x'(n)\right)^2}{\sum_n \left(x(n)\right)^2}} \tag{1}$$

$$\text{RMSE} = \sqrt{\frac{\sum_n \left(x(n) - x'(n)\right)^2}{N}} \tag{2}$$

$$\text{CR} = \frac{\text{No of uncompressed bits}}{\text{No of bits compressed bits}} \tag{3}$$

where $x'(n)$ is the reconstructed sample from lossy compressed data, $x(n)$ is original sample and N is the number of samples in the ECG record. Table I shows the summary of ECG compression performance for selected MIT/BIH recordings. The offset in ADC output was removed before estimating CR. The average values of performance parameters for all recordings are given in Table II. The proposed algorithm achieves an average lossless compression ratio of 2.1x with the test data. A lossy compression ratio of 7.86x with 0.51% PRD and RMS error of 4.61 is achieved by storing a fraction of the original data. Fig. 12 shows PRD versus lossy CR plots for a few specific MIT records.

TABLE I
COMPRESSION PERFORMANCE OF THE PROPOSED ALGORITHM WITH 5 RECORDS OF MIT/BIH DATABASE

Tape	RMSE	PRD	Lossy CR	Lossless CR
100	4.4213	0.47614	9.4334	2.2129
101	4.4231	0.47728	9.5465	2.2507
102	4.537	0.51244	9.6406	2.2251
103	4.812	0.55021	7.6608	2.1061
104	4.5783	0.53418	7.5377	2.1161

TABLE II
AVERAGE COMPRESSION PERFORMANCE OF THE PROPOSED ALGORITHM WITH 48 RECORDS OF MIT/BIH DATABASE

Avg. RMSE	Avg. PRD	Avg. Lossy CR	Avg. Lossless CR
4.61	**0.51**	**7.86**	**2.11**

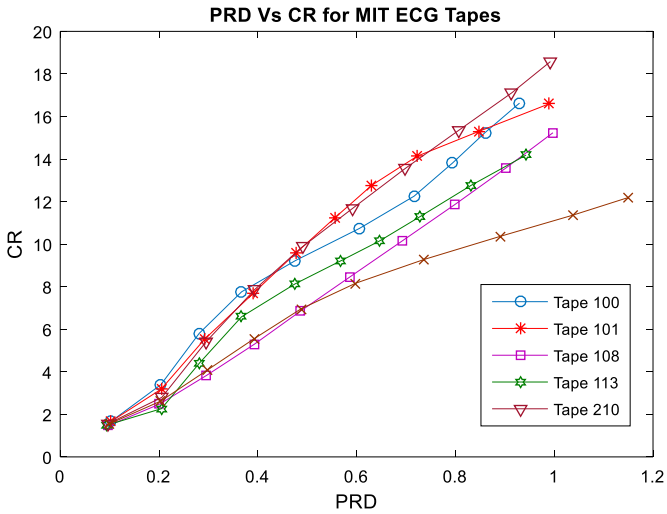

Fig. 12. PRD versus lossy compression ratio.

Table III compares the performance of existing software implemented lossy/lossless algorithms with the proposed one. The proposed scheme has low implementation complexity (as described in Section V) and enables novel data transmission techniques for power reduction (as described in Section II), and is not intended to compete with existing lossy/lossless techniques purely on compression performance. As shown, the proposed algorithm achieves a PRD of 0.51 for lossy compression at a CR of 7.8. Including the residual bits for full restoration, a lossless CR of 2.1 is achieved. Existing algorithms which uses transform domain techniques like Wavelets, DCT, Fourier transforms obtains higher lossy CRs at the expense of higher reconstruction error (PRD) and implementation complexity [7], [24], [25]. Similarly the neural networks based approach is able to achieve a higher lossy CR, but at higher PRD [27]. It is noted that these methods have been implemented only in software and is not suitable for low power sensors in IoT applications due to their complexity. Methods using SPIHT and Cubic Hermitian have similar lossy CR performance, but at higher PRD [6], [26]. For lossless compression, transform domain based Burrows Wheeler approach achieves a high CR of 3.07 at the expense of complexity, and is only implemented in software [28]. JQDC based lossless scheme proposed in [15] has slightly higher CR but higher complexity. Unlike the above methods, the proposed scheme simultaneously generates a lossy and incremental lossless stream to enable hybrid transmission and has low hardware complexity, which makes it better suited for wearable sensors in IoT applications.

TABLE III
PERFORMANCE COMPARISON WITH OTHER SOFTWARE TECHNIQUES

Method	C. R (Lossy)	C.R (Lossless)	PRD	Ref
Fourier Decomposition	17-44		0.8-2	[7]
DCT Compression	27.90	-	2.93	[24]
Wavelet with Quality Control	11.10	-	2.99	[25]
SPIHT	8.40	-	6.58	[26]
Neural Networks	18.27	-	1.17	[27]
Cubic Hermitian	2-6.6		0.9-9.6	[6]
Burrows- Wheeler	-	3.07	-	[28]
JQDC Scheme	-	2.28	-	[15]
Proposed method	7.8	2.11	0.51	-

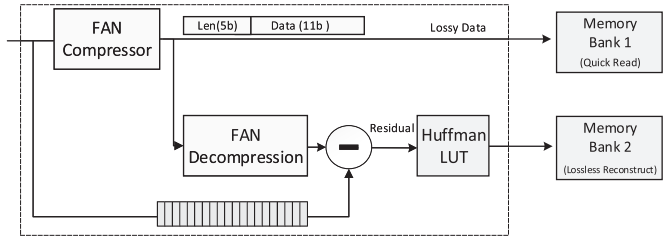

Fig. 13. Hardware architecture.

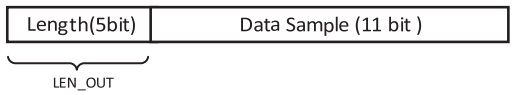

Fig. 14. Fan compressor data output format.

V. HARDWARE IMPLEMENTATION

This section describes the hardware architecture and implementation of the proposed algorithm aimed at an ECG SoC to be used in wearable sensors. The hardware architecture block diagram is given in Fig. 13.

The Fan compressor selects intermittent samples in such a way that the maximum error in reconstruction is lower than the maximum allowed error (ε). The compressor output is 16 bits wide, as shown in Fig. 14.

The 5-bit MSB is a length field (LEN_OUT) which indicates the duration between the last stored sample and the current stored sample. A linear interpolator is used to reconstruct the ECG samples based on the last two stored samples. Further, the reconstructed data is subtracted from the actual samples to compute the residuals. The maximum duration between two permanent samples (LEN_MAX) is limited to twenty. This is to limit the storage requirement of original data samples needed for computing the residuals.

A. Fan Compressor Architecture

There is no known hardware architecture reported in literature for Fan algorithm. A straight forward implementation of Fan algorithm will require the slopes of all points from

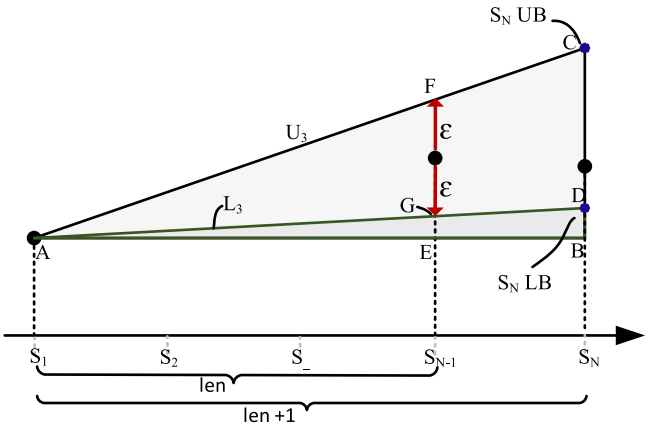

Fig. 15. Fan algorithm implementation.

the last origin point to be stored and its projections on the current sample to be calculated as described in Section III. We developed a simple recursive geometric approach for implementing Fan where only the most stringent slope and its projections are estimated/stored to simplify the calculations and reduce implementation complexity. As shown in Fig. 15, S_1 is the current origin sample, S_{N-1} is the current sample under consideration for elimination, S_N is the next sample, and "*Len*" is the duration from current origin sample to current sample S_{N-1}. In order to decide whether S_{N-1} should be kept or eliminated, the value of the slope from current origin S_1 to $S_{N-1} \pm \varepsilon$ at S_N, i.e., S_NUB and S_NLB has to be computed. This is done by considering the right triangles ABC and ABD in Fig. 15, as given in (4)–(7).

$$\text{BC} = \text{AB}.\frac{\text{EF}}{\text{AE}} = \frac{\text{Len}+1}{\text{Len}}(S_{N-1} + \varepsilon - S_1) \quad (4)$$

$$S_N\text{UB} = S_1 + \text{BC} \quad (5)$$

$$\text{BD} = \text{AB}.\frac{\text{EG}}{\text{AE}} = \frac{\text{Len}+1}{\text{Len}}(S_{N-1} - \varepsilon - S_1) \quad (6)$$

$$S_N\text{LB} = S_1 + \text{BD} \quad (7)$$

If the amplitude of S_N is not within the upper and lower bounds S_NUB and S_NLB, then the current sample S_{N-1} is chosen to be the next origin sample. Else, the current sample is eliminated. The bounds are recursively checked against the past values to select the most stringent slopes for the next sample. This way only one set of computation need to be done per sample and it simplifies the hardware. The hardware architecture of the Fan compressor is shown in Fig. 16. Due to the geometric approach, the architecture has low complexity and requires only three sets of data registers and a few combinational logic circuits for its implementation.

The ECG data samples are serially loaded into shift register marked S_N, S_{N-1}, and S_1. S_1 register stores the current origin sample S_{N-1} stores the current sample under consideration for elimination or storage and S_N stores the immediate next sample. The top half and bottom half of the circuit in Fig. 16 are similar and is used computing the upper bound $(S_N\text{UB})$ and lower bound $(S_N\text{LB})$ respectively as given in (5), (7). During

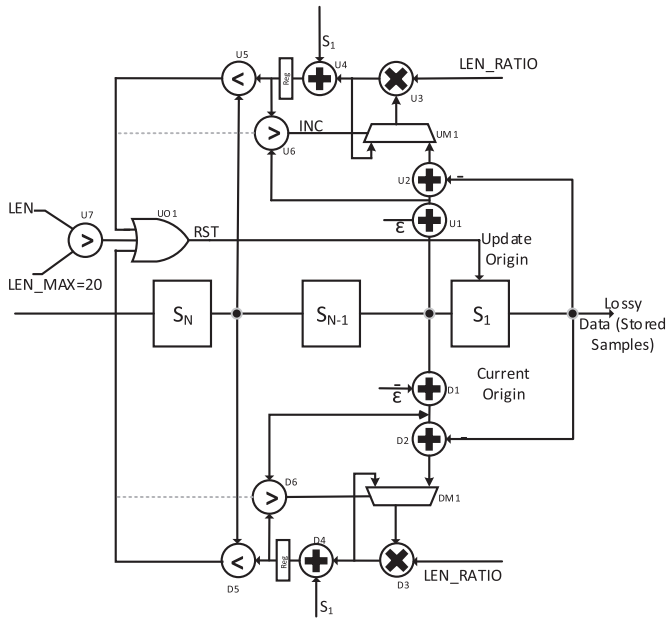

Fig. 16. Fan compressor architecture.

initialization phase the first sample is considered as origin sample and stored in S_1 register. The 2nd and 3rd ECG samples are loaded into S_{N-1} and S_N registers respectively. Adders U1, U2 and multiplier U3 is used to compute side BC of the triangle (Fig. 15) using (4). Similarly, BD (Fig. 15) is calculated using (6) using the bottom mirror of the circuit in Fig. 16. Adder U4, D4 implements (5), (7) for computing S_NUB, S_NLB which are marked in Fig. 15. Since sample stored in register S_N is within the bounds as computed by comparators U5 and D5 (as in Fig. 15) sample stored in register S_{N-1} is ignored and the next sample is serially shifted through S_N. As described in Section III every time a sample is ignored, the bounds have to recursively examined to find the most stringent bound for the next sample. This is done by comparing the bounds from maximum allowed error (i.e $S_N \pm \varepsilon$) and the prior projections on the current sample if any, from an ignored sample. This functionality of recursive checking is facilitated by comparator U6 and multiplexer UM1 for the upper bound and the equivalent components in the lower half for the lower bound. In case the current sample S_N is not within the projections of the bounds computed at the input of comparator U5, then sample under consideration (i.e., from the register S_{N-1}) is made the next origin sample and shifted to register S_1. This is enable by gate UO1 in the upper half of the circuit. The proposed geometric approach and its hardware implementation as described above enables in-place assessment of each sample and minimizes hardware requirements.

A counter is used to count the duration of the current sample from the last origin (stored) sample. Every time a sample is eliminated, the counter is incremented. If a sample converted to a stored sample, the duration of the sample from the last sample (LEN_OUT) will be passed to the counter output.

Length ratio calculation involves division operation. Since divider is costly in hardware we implemented it using a lookup table as shown in Fig. 17.

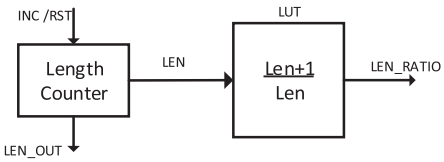

Fig. 17. Length ratio look up table.

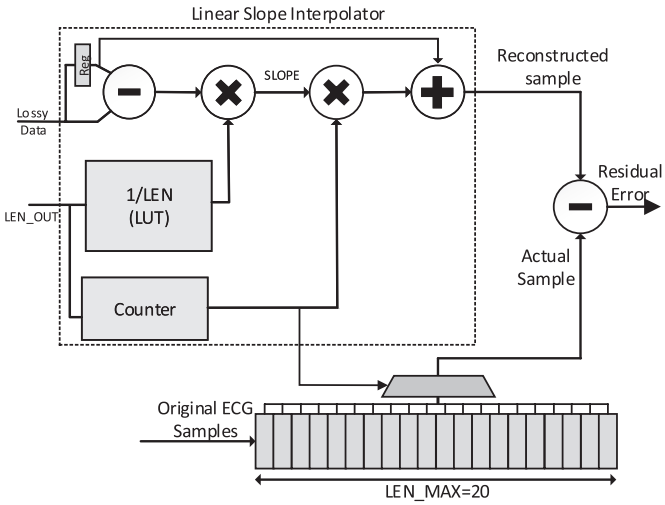

Fig. 18. Fan decompression and residue computation.

B. Fan De-Compressor Architecture

Fan de-compressor is implemented as a linear slope interpolator. The duration of the current sample from previous sample is appended along with the current sample, and is used for computing the slope of the line joining the two samples. Further, the slope is multiplied with corresponding index positions generated using a counter and added to previous sample to reconstruct the corresponding data sample. The original ECG samples are stored into a temporary register for residue computation. Based on the duration between samples, a counter is used to select the corresponding actual sample from a register array. The hardware architecture of the de-compressor and residual error calculator is shown in Fig. 18.

C. Huffman Encoder

Huffman encoder is implemented as a simple lookup table. Based on the error symbol, the corresponding statistical Huffman code is selected from the table. In this implementation ε is chosen as 10, and hence only 21 entries ($-\varepsilon$ to $+\varepsilon$) are required in the table.

D. Implementation Results

The proposed approach has been implemented in an ECG chip using 0.35 μm CMOS process based on standard cell design methodology. A Verilog RTL implementation of the proposed architecture has been developed and tested with test data generated from fixed point Matlab simulation. The design was synthesized, placed & routed, RC extracted using Synopsys Design Compiler and Cadence Encounter. The post layout results were verified and circuit power has been calculated using MIT test data.

TABLE IV
COMPARISON OF COMPRESSOR WITH OTHER HARDWARE IMPLEMENTED DESIGNS

	S.L.Chen et. al[29]	Ericson et al[13]	S.L.Chen et al [19]	C. J Deepu et al [12]	This design
Process	0.18µm	65nm	0.18µm	0.35µm	0.35µm
Vdd	1.8V	1.0V	1.8 V	2.4 V	3V
CR (lossless/lossy)	1.92/-	2.38/-	2.43/-	2.25/-	2.1/7.8
Gatecount	13.4K	53.9K	3.57K	2.26K	3.98K
Power	50µW	170µW	36.4µW	535nW	260nW

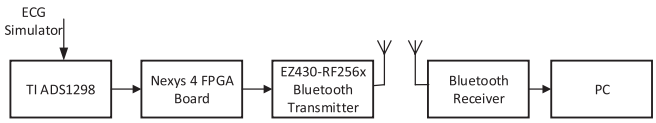

Fig. 19. Block diagram of the prototyping setup.

Comparison of the proposed compressor hardware with other recent ECG lossless compressors is given in Table IV. Among the compared, only the proposed design offers *hybrid mode transmission* capability and data rate scalability. The proposed design achieves the lowest power of 260 nW with a negligible reduction in compression ratio. Out of the total, roughly 32% is static power and the remaining is dynamic power. [13] has better compression ratio, but consumes much higher power due to the implementation of Golomb coding scheme. [19] uses selective Huffman coding scheme and consumes much higher power. Overall, the proposed design offers the lowest power for compression. As shown in next section, the proposed compression scheme implemented for a Bluetooth transceiver achieves significant power savings in wireless sensors.

VI. VERIFICATION OF PROPOSED SCHEME

A prototyping system, as shown in Fig. 19, was developed to verify the proposed compression technique.

We used a Cardiosim II ECG Simulator, TI ADS1298ECGFE-PDK ECG acquisition kit for ECG data acquisition, Digilent Nexys 4 FPGA board for implementing proposed compression scheme, and TI EZ430-RF256x Bluetooth transceiver kit for wireless communication. The current consumption of Bluetooth transceiver is measured for evaluation.

The EZ430-RF256x Bluetooth evaluation board comes with a dual mode Panasonic Bluetooth module which has Bluetooth classic and Bluetooth Low Energy radio integrated. We used the Bluetooth Low Energy mode for testing. It was noted in [30], that the power consumption of a Bluetooth device can be significantly lowered by applying manual duty cycling. Therefore, we configured the transmitter to send ECG samples from the FPGA board (compressed/uncompressed), based on duty cycles. The connection interval of Bluetooth transceiver was adjusted to support the maximum data rate required in each case. The compressed data received is decompressed by Matlab running on a PC for signal reconstruction. The current drawn by the Bluetooth module is measured using an oscilloscope with a current sensing probe. Measurements are taken when uncompressed and compressed data are being transmitted for comparison purposes. The prototyping setup

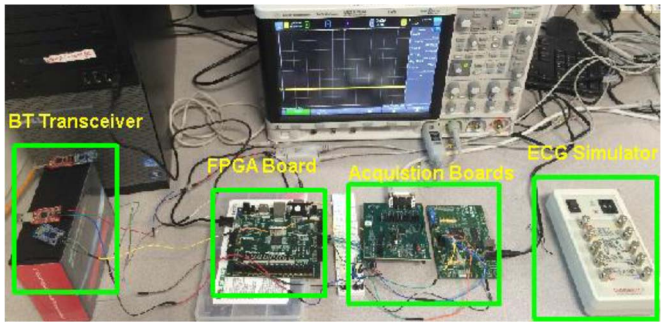

Fig. 20. Prototyping setup.

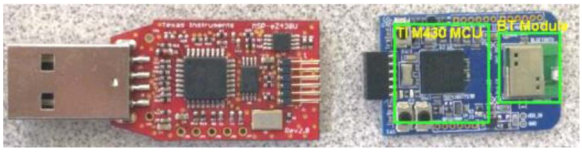

Fig. 21. TI EZ430-RF256x Bluetooth transceiver kit.

TABLE V
CURRENT CONSUMED BY BLUETOOTH AT DIFFERENT DUTY CYCLES

Duty Cycle	Compression Type	Current Consumed for Wireless Transmission
Real time	Not compressed	1.883mA
Real time	Lossless	0.988mA
Real time	Lossy	0.335mA
5s	Not compressed	1.799mA
5s	Lossless	0.921mA
5s	Lossy	0.209mA
10s	Not compressed	1.753mA
10s	Lossless	0.879mA
10s	Lossy	0.167mA

is shown in Fig. 20. We observed that the Bluetooth evaluation board is drawing an average base current of 6.5 mA when no wireless data transmission is conducted. Since the datasheet of the Bluetooth chip used (i.e TI CC2560) reveals the sleep/scan current is around $\sim$ 100 μA, we hypothesize that this base current is primarily consumed by various processes running on the MSP430 MCU and related circuitry in the same board. The Bluetooth kit we used is shown in Fig. 21. The Panasonic Bluetooth module and MSP430 MCU are marked in green color.

To get a realistic estimate of current consumed by the Bluetooth board for wireless transmission, we subtracted the base current from the measured current. The resultant currents for different duty cycles are shown in Table V. It can be observed from the table that transmission of lossy compressed data in real-time consume $\sim$18% power compared to transmission of uncompressed data stream. While losslessly compressed data requires $\sim$53% power compared to uncompressed data stream. The compression block itself consumes < 1 μA when implemented in an ECG SoC (Table IV) [12] and therefore is negligible in comparison with the system power. If the use case of the device can accept near-real time (i.e., with duty cycles of 5–10 s) data access, then the power consumption can be further reduced as shown in Table V.

VII. CONCLUSION

This paper presents a novel data compression scheme that enables *hybrid transmission mode* for balanced data quality and power consumption. The proposed scheme encodes the raw data using a lossy technique and the residual error from reconstruction is coded for lossless restoration. Applied to ECG, the scheme achieves an overall lossless compression ratio of 2.1x and a lossy compression ratio of 7.8x. The proposed scheme can be implemented either in sensor software or on-chip hardware and can be extended to other physiological signals and wireless sensors. The scheme is compatible with any combination of lossy and lossless techniques and the results may be improved by using other combinations. The hardware implementation consumes just 260 nW when synthesized in 0.35 μm CMOS process. The benefits of the proposed scheme which are demonstrated in an FPGA prototype, shows low complexity and significant power reduction and therefore is highly suited for wireless wearable sensors.

REFERENCES

[1] Y. Lian, "Challenges in design wearable wireless sensors in healthcare IoT," in *Proc. 11th IEEE Int. Conf. ASIC*, Chengdu, China, 2015, pp. 1–4.
[2] X. Zou, X. Xu, L. Yao, and Y. Lian, "A 1-V 450-nW fully integrated programmable biomedical sensor interface chip," in *IEEE J. Solid-State Circuits*, 2009, vol. 44, no. 4, pp. 1067–1077.
[3] M. Khayatzadeh, X. Zhang, J. Tan, W.-S. Liew, and Y. Lian, "A 0.7-V 17.4-/spl mu/W 3-lead wireless ECG SoC," *IEEE Trans. Biomed. Circuits Syst.*, vol. 7, no. 5, pp. 583–592, Oct. 2013.
[4] C. I. Ieong, P. I. Mak, C. P. Lam, C. Dong, M. I. Vai, P. U. Mak, S. H. Pun, F. Wan, and R. P. Martins, "A 0.83-μW QRS detection processor using quadratic spline wavelet transform for wireless ECG acquisition in 0.35-μm CMOS," *IEEE Trans. Biomed. Circuits Syst.*, vol. 6, no. 6, pp. 586–595, 2012.
[5] C. J. Deepu, X. Xu, X. Zou, L. Yao, and Y. Lian, "An ECG-on-chip for wearable cardiac monitoring devices," in *Proc. 5th IEEE Int. Symp. Electron. Des. Test Appl.*, 2010, pp. 225–228.
[6] T. Marisa, T. Niederhauser, A. Haeberlin, R. Wildhaber, R. Vogel, M. Jacomet, and J. Goette, "Bufferless compression of asynchronously sampled ECG signals in cubic Hermitian vector space," *IEEE Trans. Biomed. Eng.*, vol. 62, no. 12, pp. 2878–2887, 2015.
[7] J. Ma, T. Zhang, and M. Dong, "A novel ECG data compression method using adaptive fourier decomposition with security guarantee in e-Health applications," *IEEE J. Biomed. Heal. Inform.*, vol. 19, no. 3, pp. 1–1, 2014.
[8] H. Mamaghanian, N. Khaled, D. Atienza, and P. Vandergheynst, "Compressed sensing for real-time energy-efficient ECG compression on wireless body sensor nodes," *IEEE Trans. Biomed. Eng.*, vol. 58, no. 9, pp. 2456–2466, Sep. 2011.
[9] "Guidance for Industry: Diagnostic ECG Guidance," FDA. [Online]. Available: http://www.fda.gov/RegulatoryInformation/Guidances/ucm073942.htm
[10] "Diagnostic electrocardiographic devices," *ANSI/AAMI EC111991/(R) 2001 Assoc. Adv. Med. Instrum*.
[11] X. Zhang and Y. Lian, "A 300-mV 220-nW event-driven ADC with real-time QRS detection for wearable ECG sensors," *IEEE Trans. Biomed. Circuits Syst.*, vol. 8, no. 6, pp. 834–843, Dec. 2014.
[12] C. J. Deepu, X. Zhang, W.-S. Liew, D. L. T. Wong, and Y. Lian, "An ECG-on-chip with 535 nW/channel integrated lossless data compressor for wireless sensors," *IEEE J. Solid-State Circuits*, vol. 49, no. 11, pp. 2435–2448, 2014.
[13] E. Chua and W. Fang, "Mixed bio-signal lossless data compressor for portable brain-heart monitoring systems," *IEEE Trans. Consum. Electron.*, vol. 57, no. 1, pp. 267–273, 2011.
[14] C. J. Deepu and Y. Lian, "A low complexity lossless compression scheme for wearable ECG sensors," in *Proc. IEEE Int. Conf. Digital Signal Processing*. 2015, pp. 449–453.
[15] C. J. Deepu and Y. Lian, "A joint QRS detection and data compression scheme for wearable sensors," *IEEE Trans. Biomed. Eng.*, vol. 62, no. 1, pp. 165–175, 2015.

[16] A. L. Goldberger, L. A. N. Amaral, L. Glass, J. M. Hausdorff, P. C. Ivanov, R. G. Mark, J. E. Mietus, G. B. Moody, C.-K. Peng, and H. E. Stanley, "PhysioBank, PhysioToolkit, and PhysioNet: Components of a new research resource for complex physiologic signals," *Circulation*, vol. 101, no. 23, pp. e215–e220, Jun. 2000.
[17] C. J. Deepu, X. Zhang, W.-S. Liew, D. L. T. Wong, and Y. Lian, "Live demonstration: An ECG-on-chip for wearable wireless sensors," in *Proc. IEEE Asia Pacific Conf. Circuits and Systems*, 2014, vol. 4, pp. 177–178.
[18] D. R. Zhang, C. J. Deepu, X. Y. Xu, and Y. Lian, "A wireless ecg plaster for real-time cardiac health monitoring in body sensor networks," in *Proc. IEEE Biomedical Circuits and Systems Conf.*, 2011, pp. 205–208.
[19] S.-L. Chen and J.-G. Wang, "VLSI implementation of low-power cost-efficient lossless ECG encoder design for wireless healthcare monitoring application," *Electron. Lett.*, vol. 49, no. 2, pp. 91–93, Jan. 2013.
[20] S. M. S. Jalaleddine, C. G. Hutchens, R. D. Strattan, and W. A. Coberly, "ECG data compression techniques-a unified approach," *IEEE Trans. Biomed. Eng.*, vol. 37, no. 4, pp. 329–343, Apr. 1990.
[21] I. Banville and S. Armstrong, "Quantification of real-time ECG data compression algorithms," in *Proc. IEEE Engineering in Medicine and Biology 21st Annu. Conf.*, 1999, vol. 1, p. 264.
[22] S. M. Blanchard and R. C. Barr, "Comparison of methods for adaptive sampling of cardiac electrograms and electrocardiograms," *Med. Biol. Eng. Comput.*, vol. 23, no. 4, pp. 377–386, 1985.
[23] Y. Zou, J. Han, S. Xuan, S. Huang, X. Weng, D. Fang, and X. Zeng, "An energy-efficient design for ECG recording and R-peak detection based on wavelet transform," *IEEE Trans. Circuits Syst. II: Express Briefs*, vol. 62, no. 2, pp. 119–123, 2015.
[24] S. Lee, J. Kim, and M. Lee, "A real-time ECG data compression and transmission algorithm for an e-health device," *IEEE Trans. Biomed. Eng.*, vol. 58, no. 9, pp. 2448–2455, 2011.
[25] C.-T. K. C.-T. Ku, K.-C. H. K.-C. Hung, T.-C. W. T.-C. Wu, and H.-S. W. H.-S. Wang, "Wavelet-based ECG data compression system with linear quality control scheme," *IEEE Trans. Biomed. Eng.*, vol. 57, no. 6, pp. 1399–1409, 2010.
[26] A. Alesanco and J. Garcia, "Automatic real-time ECG coding methodology guaranteeing signal interpretation quality," *IEEE Trans. Biomed. Eng.*, vol. 55, no. 11, pp. 2519–2527, Nov. 2008.
[27] C. M. Fira and L. Goras, "An ECG signals compression method and its validation using NNs," *IEEE Trans. Biomed. Eng.*, vol. 55, no. 4, pp. 1319–1326, Apr. 2008.
[28] Z. Arnavut, "ECG signal compression based on burrows-wheeler transformation and inversion ranks of linear prediction," *IEEE Trans. Biomed. Eng.*, vol. 54, no. 3, pp. 410–418, Mar. 2007.
[29] S. S.-L. Chen, H. H.-Y. Lee, C. C.-A. Chen, H.-Y. Huang, and C.-H. Luo, "Wireless body sensor network with adaptive low-power design for biometrics and healthcare applications," *IEEE Syst. J.*, vol. 3, no. 4, pp. 398–409, Dec. 2009.
[30] A. Dementyev, S. Hodges, S. Taylor, and J. Smith, "Power consumption analysis of Bluetooth Low Energy, ZigBee and ANT sensor nodes in a cyclic sleep scenario," in *Proc. IEEE Int. Wireless Symp.*, 2013, pp. 2–5.
[31] D. John, Z. Xiaoyang, C. Heng, and L. Yong, "A 3-lead ECG-on-chip with QRS detection & lossless compression for wireless sensors," *IEEE Trans. Circuits Syst. II, Exp. Briefs*, 2016, doi: 10.1109/TCSII.2016.2613564.

Chacko John Deepu (S'07–M'14–SM'15) received the B.Tech. degree in electronics and communication engineering from the University of Kerala, Thiruvananthapuram, India, in 2002, and the M.Sc. and Ph.D. degrees in electrical engineering from the National University of Singapore (NUS), Singapore, in 2008 and 2014, respectively.

He is a postdoctoral researcher at the Bioelectronics Laboratory, National University of Singapore. Previously, he worked as a Senior Engineer at Sanyo Semiconductors (2004–2006) and as a Design Engineer at Ushus Technologies (2002–2004). His research interests include energy efficient signal processing, low power biomedical circuit design, and wearable healthcare devices.

Dr. Deepu was the recipient of the Institution of Engineers Singapore Prestigious Engineering Achievement Award in 2011, Best Design Award at the Asian Solid State Circuit Conference in 2013, and the IEEE Young Professionals, Region 10 individual award in 2013. He served as a member of technical program committee for IEEE conferences TENCON 2009, ASICON 2015, and TENCON 2016.

Chun-Huat Heng (S'96–M'04–SM'13) received the B.Eng. and M.Eng. degrees from the National University of Singapore (NUS), Singapore, in 1996 and 1999, respectively, and the Ph.D. degree from the University of Illinois at Urbana-Champaign, Urbana, IL, USA, in 2003.

He has been working on CMOS integrated circuits involving synthesizer, delay-locked loop, and transceiver circuits. From 2001 to 2004, he was with Wireless Interface Technologies, which was later acquired by Chrontel. Since 2004, he has been with NUS, where he is currently an Associate Professor.

Dr. Heng has received the NUS Annual Teaching Excellence Award in 2008, 2011, and 2013, and was on the ATEA Honor Roll in 2014. Also, he has won the Faculty Innovative Teaching Award in 2009. He was an Associate Editor for IEEE TRANSACTIONS ON CIRCUITS AND SYSTEMS II, and is currently a Technical Program Committee member for International Solid-State Circuits Conference and Asian Solid-State Circuits Conference.

Yong Lian (M'90–SM'99–F'09) received the B.Sc. degree from the College of Economics and Management, Shanghai Jiao Tong University, Shanghai, China, in 1984, and the Ph.D. degree from the Department of Electrical Engineering, National University of Singapore (NUS), Singapore, in 1994.

In 1996, after spending nine years in industry, he joined NUS, where he was appointed as the first Provost's Chair Professor in the Department of Electrical and Computer Engineering in 2011. Currently, he is a Professor in the Department of Electrical Engineering and Computer Science, Lassonde School of Engineering, York University, Toronto, ON, Canada. His research interests include biomedical circuits and systems and signal processing.

Dr. Lian's research has received many awards, including the IEEE Circuits and Systems Society's Guillemin-Cauer Award in 1996, the IEEE Communications Society Multimedia Communications Best Paper Award in 2008, the Institution of Engineers Singapore Prestigious Engineering Achievement Award in 2011, the Hua Yuan Association/Tan Kah Kee International Society Outstanding Contribution Award in 2013, the Chen-Ning Franklin Yang Award in Science and Technology for New Immigrant in 2014, and the Design Contest Award at the 20th International Symposium on Low Power Electronics and Design in 2015. As an educator, he received the University Annual Teaching Excellent Award in two consecutive academic years from 2008 to 2010 and many other teaching awards from the Faculty of Engineering. Under his guidance, his students received many awards, including the Best Student Paper Award in ICME 2007, winner of 47th DAC/ISSCC Student Design Contest in 2010, and the Best Design Award in A-SSCC 2013 Student Design Contest. He is the President-Elect of the IEEE Circuits and Systems (CAS) Society, a Steering Committee Member of the IEEE TRANSACTIONS ON BIOMEDICAL CIRCUITS AND SYSTEMS. He was the Editor-in-Chief of the IEEE TRANSACTIONS ON CIRCUITS AND SYSTEMS PART II: EXPRESS BRIEFS for two terms from 2010 to 2013. He was the Guest Editor for eight special issues in the IEEE TRANSACTIONS ON CIRCUITS AND SYSTEMS-PART I: REGULAR PAPERS, the IEEE TRANSACTIONS ON BIOMEDICAL CIRCUITS AND SYSTEMS, and the *Journal of Circuits, Systems Signal Processing*. He was the Vice President for Publications of the IEEE CAS Society from 2013 to 2015, the Vice President for the Asia Pacific Region of the IEEE CAS Society from 2007 to 2008, an AdComm Member of the IEEE Biometrics Council from 2008 to 2009, the CAS Society Representative to the BioTechnology Council from 2007 to 2009, the Chair of the BioCAS Technical Committee of the IEEE CAS Society from 2007 to 2009, the Chair of the DSP Technical Committee of the IEEE CAS Society from 2010 to 2011, a member of the IEEE Medal for Innovations in Healthcare Technology Committee from 2010 to 2012, and a Distinguished Lecturer of the IEEE CAS Society from 2004 to 2005. He is the Founder of the International Conference on Green Circuits and Systems, the Asia Pacific Conference on Postgraduate Research in Microelectronics and Electronics, and the IEEE Biomedical Circuits and Systems Conference. He is a Fellow of the Academy of Engineering Singapore.